



Cryogenic rolling shear characteristics of birch plywood for LNG cargo containment systems

Hee-Tae Kim¹ · Ki-Young Sung² · Jeong-Hyeon Kim[†] · Jae-Myung Lee^{††}

(Received October 20, 2025 ; Revised November 11, 2025 ; Accepted December 22, 2025)

Abstract: Birch plywood is widely used as a reinforcement material in the insulation panels of liquefied natural gas (LNG) cargo containment systems (CCS) to protect polyurethane foam (PUF) insulation from mechanical damage. The plywood must endure in-plane shear stresses generated by sloshing impacts, thermal contraction, and loads transferred through mastic ropes and anchoring plates. In this study, a cryogenic rolling shear test apparatus was designed to evaluate the in-plane shear properties of birch plywood under cryogenic conditions, focusing on the effect of panel thickness. Test results indicated that 12 mm thick plywood exhibited lower in-plane shear strength than 9 mm thick plywood. Furthermore, cryogenic conditions increased the in-plane shear strength of the 9 mm panels but reduced that of the 12 mm panels. The 9 mm plywood also showed pronounced anisotropic behavior depending on the grain orientation of the outer veneer layers, whereas this anisotropy diminished in the 12 mm panels.

Keywords: Plywood, Rolling shear, Cryogenic, LNG cargo containment system

1. Introduction

The cargo containment system (CCS) of liquefied natural gas (LNG) carriers, such as the NO.96 and Mark III membrane type systems, is responsible for bearing the cargo load and maintaining cryogenic integrity at $-163\text{ }^{\circ}\text{C}$ [1]. These systems were developed to meet the growing global demand for natural gas, with the insulation structure typically a plywood–polyurethane foam sandwich panel serving both thermal and mechanical functions by directly supporting the cargo load.

In the Mark III system, birch plywood is used as the insulation support material to enhance the bending rigidity of the insulation panel made of reinforced polyurethane foam (R-PUF) and to prevent mechanical damage to the R-PUF during installation. In contrast, in the NO.96 system, plywood acts as an insulated container that holds materials such as glass wool and perlite, thereby ensuring the overall structural integrity of the CCS [2].

In both systems, the bottom plywood layer is bonded to the hull via mastic ropes and typically operates at ambient temperature. During vessel operation, hull motions and ballast pressure generate in-plane shear stresses in the mastic bonding region.

Additionally, bending deformation between the mastic ropes induced by sloshing impacts causes further in-plane shear strains. Consequently, structural verification of the birch plywood is required to evaluate the damage caused by these combined loadings [3]. Furthermore, in regions where the plywood lies directly beneath the primary barrier and comes into contact with LNG, a 3 mm-thick stainless-steel anchor plate is inserted. The anchor plate is welded to the primary barrier to maintain fixation, and thermal contraction or sloshing loads in the barrier can induce additional in-plane shear stresses in the plywood [4]. As illustrated in **Figure 1**, plywood is inherently susceptible to in-plane shear failure due to lathe checks formed during veneer manufacturing [5]. Therefore, a comprehensive evaluation of its in-plane shear strength is essential for reliable CCS design.

In onshore structural applications, extensive research has been carried out on the in-plane shear properties and failure behavior of plywood. For instance, architectural birch plywood has been experimentally investigated for its in-plane shear strength and orthotropic mechanical characteristics under tensile, compressive, and bending loads [6][7]. Numerical models incorporating in-plane

†† Co-Corresponding Author (ORCID: <http://orcid.org/0000-0002-8096-4306>): Professor, Department of Naval Architecture and Ocean Engineering, Pusan National University, 2, Busandaehak-ro 63beon-gil, Geumjeong-gu, Busan 46241, Korea, E-mail: jaemlee@pusan.ac.kr, Tel: 051-510-2342

† Corresponding Author (ORCID: <https://orcid.org/0000-0002-7336-5540>): Professor, Hydrogen Ship Technology Center, Pusan National University, 2, Busandaehak-ro 63beon-gil, Geumjeong-gu, Busan 46241, Korea, E-mail: jeonghkim@pusan.ac.kr, Tel: 051-510-7746

1 Ph. D. Candidate, Hydrogen Ship Technology Center, Pusan National University, E-mail: 201329122@pusan.ac.kr Tel: 051-510-2340

2 Senior Research Engineer, Korea Research Institute of Ships and Ocean Engineering (KRISO), E-mail: kysung@kriso.re.kr Tel: 055-639-2412

This is an Open Access article distributed under the terms of the Creative Commons Attribution Non-Commercial License (<http://creativecommons.org/licenses/by-nc/3.0>), which permits unrestricted non-commercial use, distribution, and reproduction in any medium, provided the original work is properly cited.

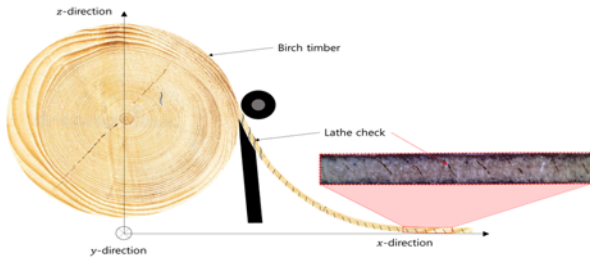


Figure 1: Schematic of a lathe-check flaw generated during the veneer manufacturing process

shear failure mechanisms have also been proposed based on these experimental results [8]. In addition, the shear failure vulnerability of birch cross-laminated timber (CLT) has been analyzed through rolling shear tests [9].

However, compared with architectural and civil engineering applications, relatively few studies have addressed the mechanical characteristics of birch plywood under cryogenic conditions relevant to LNG CCS. Previous works have examined the compressive behavior of birch plywood at cryogenic temperatures considering its orthotropic nature [1], as well as its tensile and bending strength degradation under thermal cycling [2][10]. In addition, the deterioration of compressive properties due to seawater or freshwater exposure in cryogenic environments has also been investigated [11].

Nevertheless, quantitative data on the in-plane shear characteristics of birch plywood for LNG CCS applications remain limited. Therefore, the objective of this study is to experimentally evaluate the in-plane shear properties of birch plywood and to clarify the effects of plywood thickness and grain orientation under cryogenic conditions.

2. Experimental Preparation

2.1 Preparation of Rolling Shear Test Specimens

Birch plywood supplied by Latvijas Finieris was used for this study. Two thicknesses were prepared: 9 mm plywood composed of seven veneer layers and 12 mm plywood composed of nine veneer layers. For the details, 9mm plywood direction and veneer direction are illustrated in **Figure 2**.

Figure 3 shows a schematic of the plywood rolling shear test specimen. To evaluate the in-plane shear properties of birch plywood, rolling shear tests were conducted in accordance with ASTM D2718-18, Standard Test Methods for Structural Panels in Planar Shear (Rolling Shear). According to this standard, the specimens were 150 mm in length and 50 mm in width. The loading

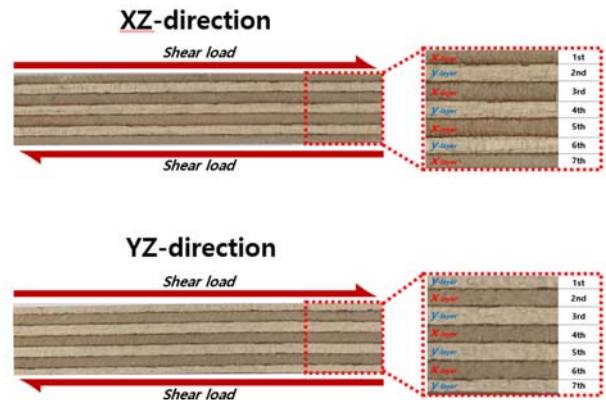


Figure 2: Plywood direction definition and shear loading direction for 9 mm plywood (7-ply)

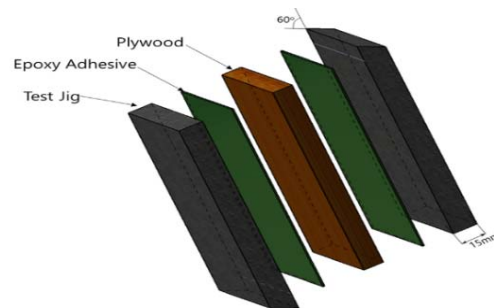


Figure 3: Schematic of the plywood rolling shear test specimen

rate was set to 0.3 mm/min, corresponding to 0.002 times the specimen length.

The preparation of the specimens and test configuration are shown in **Figure 4 (b)**. The test jig was fabricated from titanium alloy to ensure sufficient stiffness, and a cryogenic epoxy adhesive (UEA-100/300, Uni-Tech) was used to bond the plywood specimens to the titanium fixtures to avoid titanium jig-adhesive failure. The epoxy adhesive exhibits excellent cryogenic mechanical performance, with high tensile properties [12] and a shear strength of 20 MPa at $-150\text{ }^{\circ}\text{C}$ [13].

In cryogenic testing of membrane-type LNG CCS, mechanical test methods are typically based on ASTM standards but are applied using specimens made from LNG CCS structural materials. For example, Lee *et al.* (2011) studied the debonding failure characteristics of a membrane-type LNG CCS barrier system under pull-off loading using epoxy and polyurethane adhesives designed for cryogenic applications. The experiments were conducted in accordance with ASTM standards; however, the specimens were fabricated as a triplex composite–adhesive–triplex composite assembly, matching the LNG CCS structure to reflect the real structure’s thermal stresses and mechanical strength [13].

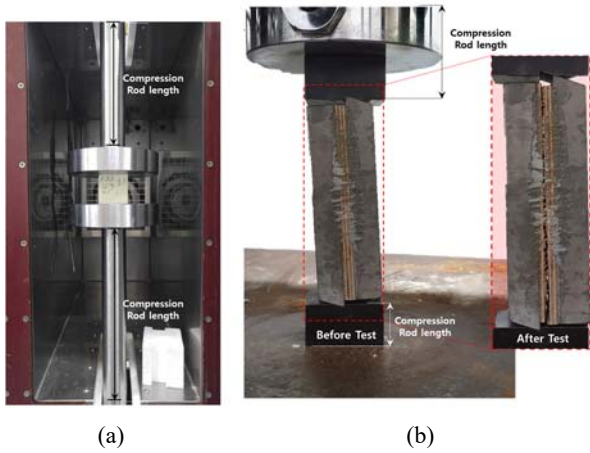


Figure 4: Conventional cryogenic compression test setup (a) and rolling shear test setup (b).

2.2 Cryogenic Test Chamber Design

In the rolling shear test, the specimen and the compression jig make line contact, unlike conventional compression tests that involve surface contact. Due to this configuration, extending the compression jig length—as commonly done in conventional cryogenic compression setups—can cause deflection perpendicular to the loading direction before shear failure occurs. To minimize or eliminate this deflection, a shorter compression jig design is required for the rolling shear test.

In this study, a novel cryogenic chamber was developed to evaluate the in-plane shear strength of birch plywood under cryogenic conditions. **Figure 5** shows a schematic cryogenic sliding chamber attached to a universal testing machine (UTM) at both room and cryogenic temperatures. To accommodate short compression rods while allowing deformation without mechanical resistance at low temperatures, the chamber was designed with two nested insulation boxes arranged in a drawer-like configuration to ensure smooth displacement. The contact and friction surfaces of the chamber were insulated with expanded polystyrene (EPS) to maintain airtightness, and PTFE films were applied to minimize friction.

The chamber temperature was controlled by injecting cryogenic nitrogen gas through a solenoid valve operating in relay mode, based on feedback from a K-type thermocouple installed inside the chamber. The relay-control system maintained the temperature within a ± 1 °C hysteresis band around the target set-point. To measure the plywood cooling time, a rolling-shear specimen was prepared with a hole at the plywood center (1.5 mm in diameter and 75 mm in depth) along the 150 mm specimen length. **Figure 6** shows the thermocouple measurement locations in the rolling-shear specimen and the corresponding time–

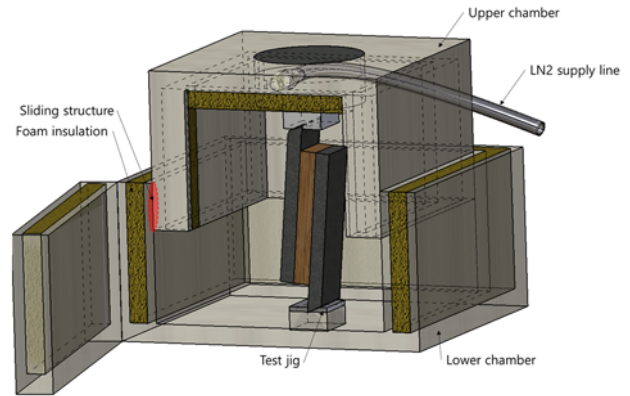


Figure 5: Schematic of the cryogenic sliding chamber for the plywood rolling shear test

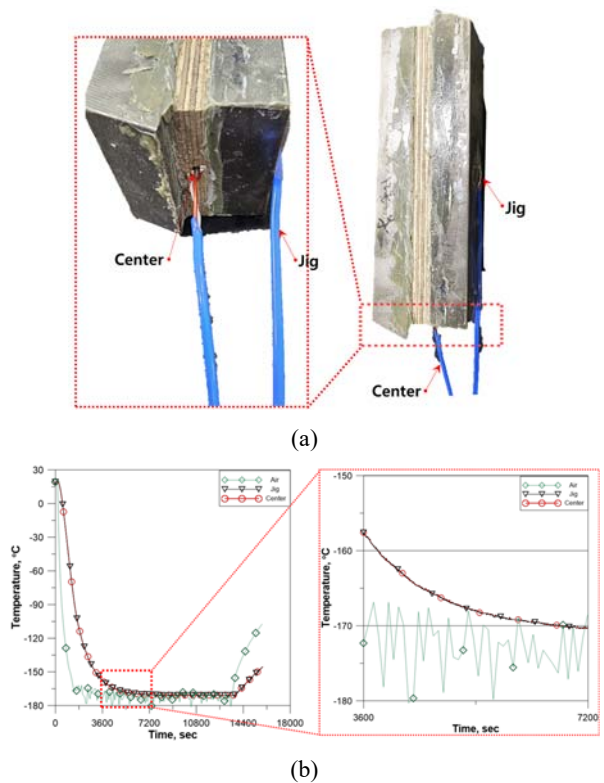


Figure 6: Thermocouple attachment on the plywood rolling shear specimen (a) and temperature histories of the plywood, titanium alloy jig, and chamber air (b).

temperature histories, together with the chamber air temperature. The specimen required approximately 2 h to reach the target temperature. Although the chamber air temperature exhibited relatively large hysteresis, the plywood and jig temperatures stabilized after about 2 h, as shown in **Figure 6**.

2.3 Rolling Shear Test Method and Scenario

Rolling shear tests were conducted at room temperature and at a cryogenic temperature of -170 °C. To account for the orthotropic characteristics of birch plywood, tests were performed in

two principal directions—XZ and YZ—with five repetitions for each condition. According to ASTM D2718-18, Standard Test Methods for Structural Panels in Planar Shear (Rolling Shear), the shear strength (f_s) and shear modulus (G) are calculated using the following equations:

$$f_s = \frac{P_{max}}{b \times L} \tag{1}$$

$$G = \frac{d}{b \times L} \frac{\Delta P}{\Delta y} \tag{2}$$

where b is the plywood width of 50 mm, d is the thickness of the specimen, L is the specimen length of 150 mm, P_{max} is the maximum load during the test, and $\Delta P/\Delta y$ is the slope of the load–deformation curve.

In the rolling shear configuration, the plywood specimen is not aligned parallel to the loading axis of the UTM but instead positioned at an acute angle. This inclination must be considered when determining the effective shear strength. The geometric correction for the initial inclination of the plywood’s longitudinal direction is illustrated in **Figure 6** [14].

The correction angle (α) is calculated as follows:

$$\alpha = \tan^{-1} \left(\frac{L - \sqrt{L^2 - 4t_0(t_0 + t_c)}}{2t_0} \right) \times \frac{180}{\pi} \tag{3}$$

Accordingly, the adjusted shear strength and shear modulus are obtained using the following expressions:

$$f_s = \frac{P_{max} \times \cos(\alpha)}{b \times L} \tag{4}$$

$$G = \frac{d}{b \times L} \frac{\Delta(P \times \cos(\alpha))}{\Delta(y \times \cos(\alpha))} \tag{5}$$

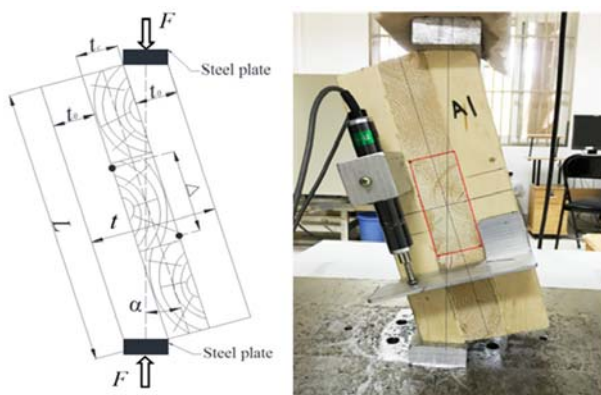


Figure 7: Rolling shear test configuration and definition of plywood angle α [14].

Table 1: Test conditions and scenarios for plywood rolling shear experiments.

Specimen	Plane direction	Temp.(°C)	No. of test
Plywood 9t	XZ	25, -170	5
	YZ		5
Plywood 12t	XZ	25, -170	5
	YZ		5

Table 1 shows the test conditions and scenarios for plywood rolling shear experiments.

3. Results and Discussion

3.1 Rolling Shear Test Results

In the evaluation of the in-plane shear failure characteristics of birch plywood, the 12 mm-thick specimens exhibited different behavior compared to the 9 mm-thick specimens in both the XZ and YZ directions at room temperature. **Figure 8** shows the Rolling shear test results for 9 mm plywood at room temperature and at cryogenic temperature. For 9 mm plywood, in room temperature, the shear strength in the XZ direction was higher than in the YZ direction. This is because, under rolling shear loading in the YZ direction, the central veneer layer oriented in the X direction which is more vulnerable to in-plane shear is positioned exactly at the specimen’s mid-plane and cannot sufficiently accommodate shear deformation, leading to failure at relatively lower strength. Under cryogenic conditions, however, fracture occurred primarily along the bonding interface between veneer layers rather than through rolling shear deformation. And thermal contraction of epoxy adhesive increase thermal stress in plywood outer veneers. And those stress cause strength degradation in XZ direction which has X-direction veneer on surface, and YZ direction relatively not affected for thermal stress of adhesive due to high strength Y-direction veneer on surface and slightly increased maximum stress to failure due to increased elastic modulus under cryogenic environment.

Figure 9 shows the rolling shear test results for 12 mm plywood at room temperature and at cryogenic temperature. As shown, the 12 mm plywood exhibited reduced orthotropic anisotropy compared with the 9 mm plywood. Since it contains a greater number of X-direction veneer layers with lathe checks—microcracks formed during the veneer manufacturing process—that are prone to in-plane shear failure, the 12 mm specimens showed lower overall strength. Among all test conditions, the 12 mm plywood under cryogenic temperature demonstrated the lowest shear strength.

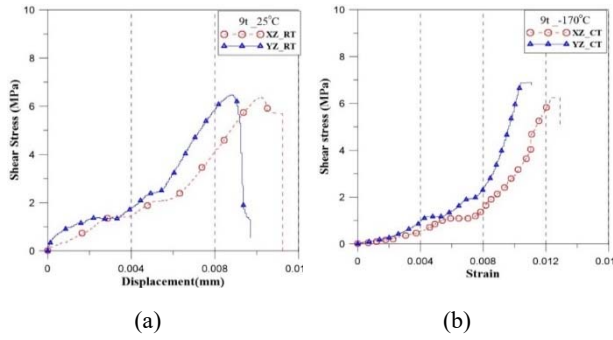


Figure 8: Rolling shear test results for 9 mm plywood at room temperature (a) and at cryogenic temperature (b)

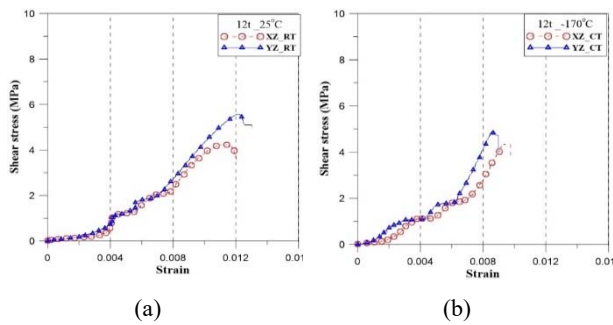


Figure 9: Rolling shear test results for 12 mm plywood at room temperature (a) and at cryogenic temperature (b)

Table 2: Summary of rolling shear test results for 9 mm plywood

No.	Case	Stress (MPa)	Strain
1	XZ, 25°C	6.39	0.0118
2		7.74	0.0111
3		6.37	0.0102
4		6.05	0.0138
5		6.21	0.0134
StDev.		0.60	0.0014
Avg.		6.55	0.0120
1	YZ, 25°C	4.86	0.0096
2		5.40	0.0096
3		6.49	0.0088
4		5.44	0.0118
5		6.31	0.0106
StDev.		0.61	0.0010
Avg.		5.70	0.0101
1	XZ, -170°C	5.81	0.0093
2		4.86	0.0120
3		6.25	0.0124
4		5.77	0.0076
5		7.11	0.0114
StDev.		0.73	0.0018
Avg.		5.96	0.0105
1	YZ, -170°C	6.72	0.0126
2		4.92	0.0078
3		5.48	0.0098
4		6.88	0.0111
5		5.85	0.0124
StDev.		0.74	0.0107
Avg.		5.97	0.0108

Table 3: Summary of rolling shear test results for 12 mm plywood

No.	Case	Stress (MPa)	Strain
1	XZ, 25°C	3.64	0.0082
2		4.25	0.0112
3		3.18	0.0094
4		3.48	0.0120
5		4.53	0.0115
StDev.			0.50
Avg.		3.82	0.0105
1	YZ, 25°C	5.33	0.0122
2		3.27	0.0110
3		4.61	0.0083
4		5.57	0.0121
5		5.70	0.0113
StDev.			0.90
Avg.		4.90	0.0110
1	XZ, -170°C	4.47	0.0070
2		3.58	0.0071
3		4.35	0.0093
4		4.18	0.0068
5		4.11	0.0097
StDev.			0.31
Avg.		4.14	0.0080
1	YZ, -170°C	4.91	0.0086
2		4.18	0.0072
3		4.05	0.0082
4		4.45	0.0092
5		5.19	0.0066
StDev.			0.43
Avg.		4.56	0.0079

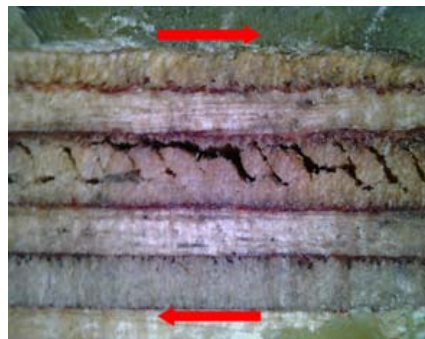
Tables 2 and 3 summarize the rolling shear test results for 9 mm and 12 mm plywood. For 9 mm plywood, distinct orthotropic behavior was observed in both room-temperature and cryogenic environments. In contrast, the 12 mm plywood exhibited nearly similar shear behavior in both XZ and YZ directions, except for minor differences in shear strength. This tendency can be explained by the increased number of lathe checks within the thicker plywood, particularly in the X-direction veneer layers perpendicular to the loading direction, which makes the material more susceptible to rolling shear. During the rolling shear tests, these lathe checks accommodated shear deformation through microcrack propagation, resulting in an initial load plateau region in the curves.

The 9 mm XZ and 12 mm YZ specimens showed quantitative similarity because both have a Y-direction center veneer, which provides higher in-plane shear stiffness; therefore, the room-temperature in-plane shear strength is relatively high. Under cryogenic conditions, however, increased thermal stress and resin embrittlement in the phenolic adhesive between veneers reduce the in-plane shear strength. In contrast, the 9 mm YZ and 12 mm XZ specimens have an X-direction center veneer, which has lower in-plane shear stiffness and thus lower shear strength at room

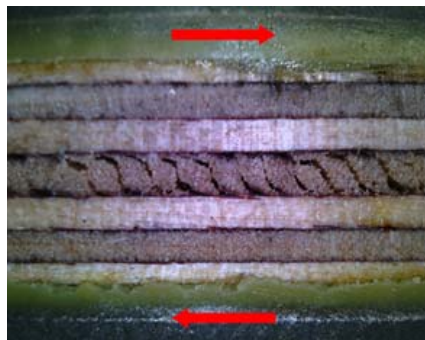
temperature. Under cryogenic conditions, increased lap shear strength makes it more difficult for lathe checks to “roll” in the X-direction veneer, resulting in an increase in cryogenic in-plane shear strength.

3.2 Rolling Shear Fracture Analysis

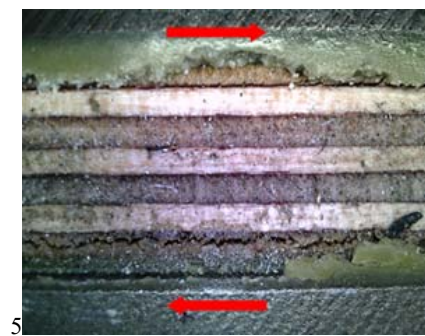
Rolling shear failure in plywood primarily occurs along lathe defects within the X-direction veneer, leading to the complete rupture of that veneer layer. The wood fibers composing the



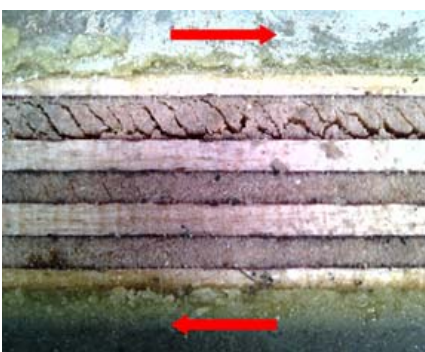
(a)



(b)



(c)



(d)

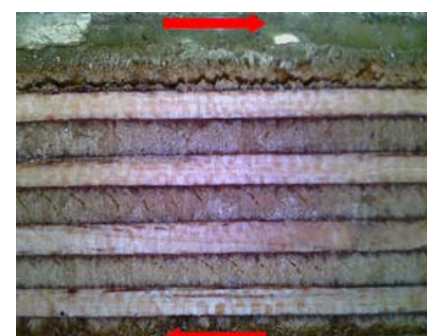
Figure 10: Rolling shear failure of 9 mm plywood at room temperature: XZ (a), YZ (b); and at cryogenic temperature: XZ (c), YZ (d)



(a)



(b)



(c)



(d)

Figure 11: Rolling shear failure of 12 mm plywood at room temperature: XZ (a), YZ (b); and at cryogenic temperature: XZ (c), YZ (d)

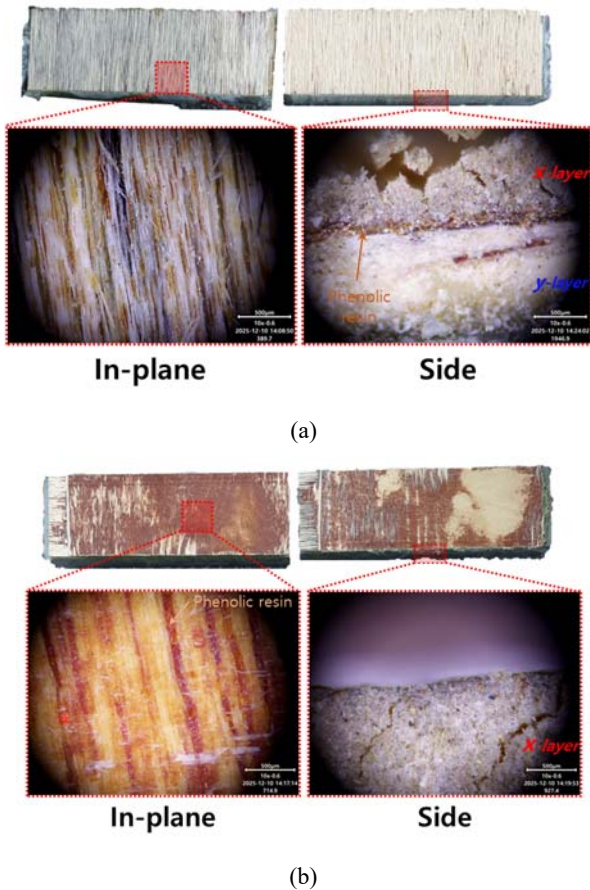


Figure 12: Microscopic analysis of rolling shear failure: veneer shear failure (a) and interfacial failure in the phenolic resin (b)

veneer separate into parallelogram-shaped fiber blocks along these lathe defect lines. While rolling shear failure can still occur along these defects under cryogenic conditions, shear failure at the bonding interfaces between veneers becomes more dominant in low-temperature environments.

Figure 10 shows the rolling shear failure of 9 mm plywood at room temperature (XZ and YZ) and cryogenic temperature (XZ and YZ). For the 9 mm plywood, at room temperature, the fracture surface developed along the lathe defect located in the central X-direction veneer of the specimen. Under cryogenic conditions, however, the failure shifted to the bonding joints between veneers, indicating the influence of adhesive embrittlement and interfacial weakening at low temperatures. For these reasons, the X-direction veneer shows rolling-shear deformation associated with lathe checks at room temperature, whereas almost no rolling-shear deformation occurs at cryogenic temperature. For example, **Figure 10(b)** shows veneer rotation between lathe checks at room temperature, while **Figure 10(d)** shows lathe checks with little to no rotation.

Figure 11 shows the rolling shear failure of 12 mm plywood

at room temperature (XZ and YZ) and cryogenic temperature (XZ and YZ). In the case of 12 mm plywood, the fracture surface was located in the outermost X-direction veneer layer, furthest from the mid-plane of the specimen, in both room-temperature and cryogenic tests. At room temperature, rolling shear failure along the lathe defect in the X-direction veneer was prominent, showing a typical in-plane shear fracture pattern. Under cryogenic conditions, however, similar to the 9 mm plywood, failure occurred mainly at the veneer-to-veneer interface, attributed to thermal stress concentration and adhesive embrittlement within the bonding region.

4. Conclusion

At room temperature, lathe checks make plywood vulnerable to in-plane shear loading in the X-direction veneer. Lathe checks accommodate shear deformation by widening cracks and by local rolling deformation. This behavior appears in the initial stagnation region of the stress–strain curve at approximately 2 MPa. Grain-direction anisotropy shows a quantitative relationship with the center-veneer orientation. For the 9 mm plywood, the XZ shear strength is higher than the YZ shear strength because the YZ configuration has an X-direction center veneer. For the 12 mm plywood, the YZ shear strength is higher than the XZ shear strength because the XZ configuration has an X-direction center veneer.

Under cryogenic temperature, phenolic resin embrittlement between veneers, together with stiffness anisotropy and differential thermal contraction, changes the dominant failure mechanism. For X-direction center-veneer cases (9 mm YZ and 12 mm XZ), the increased lap shear strength increases the rolling-shear strength by suppressing rolling deformation compared with room temperature. However, for Y-direction center-veneer cases (9 mm XZ and 12 mm YZ), the larger thermal contraction of the Y-direction veneer causes stress imbalance in the X-direction veneer during in-plane shear deformation, leading to crack initiation on one side and interfacial fracture of the phenolic resin without rolling-shear deformation.

This study experimentally evaluated the in-plane shear failure behavior of birch plywood used in LNG cargo containment systems (CCS) with respect to temperature and plywood thickness. The findings provide essential shear property data for predicting plywood failure during actual CCS operation. Furthermore, the design and implementation of a dedicated cryogenic test facility for in-plane shear evaluation in this study establish a foundation

for future research on the cryogenic mechanical behavior of plywood materials.

Acknowledgement

This research was supported by Korea Research Institute of Ships & Ocean Engineering a grant from Endowment Project of “Development of Core Technology for Offshore Green Hydrogen to Realize a Carbon-Neutral Society” funded by Ministry of Oceans and Fisheries(2520000682, PES5544). This research was supported by Development and demonstration of on-board marine debris disposal modules program of Korea Institute of Marine Science & Technology Promotion(KIMST) funded by the Ministry of Oceans and Fisheries(KIMST-20220494).

Author Contributions

Conceptualization, J. H. Kim and H. T. Kim; Methodology, J. M. Lee and H. T. Kim; Software, Investigation, K. Y. Sung; Resources, J. H. Kim; Data Curation, H. T. Kim; Writing-Original Draft Preparation, J. M. Lee and H. T. Kim; Writing-Review & Editing, H. T. Kim and K. Y. Sung; Visualization, J. H. Kim; Supervision, J. M. Lee; Project Administration, J. M. Lee; Funding Acquisition, J. H. Kim and J. M. Lee.

References

- [1] S. J. Cha, J. D. Kim, S. K. Kim, J. H. Kim, H. K. Oh, Y. T. Kim, S. B. Park, and J. M. Lee, “Effect of temperature on the mechanical performance of plywood used in membrane-type LNG carrier insulation systems,” *Journal of Wood Science*, vol. 66, no. 1, 2020.
- [2] J. H. Kim, D. H. Park, C. S. Lee, K. J. Park, J. M. Lee, “Effects of cryogenic thermal cycle and immersion on the mechanical characteristics of phenol-resin bonded plywood,” *Cryogenics*, vol. 72, no. part 1, pp. 90-102, 2015.
- [3] J. Kuo, R. Campbell, Z. Ding, S. Hoie, A. Rinehart, R. Sandström, T. Yung, M. Greer, and M. Danaczko, “LNG tank sloshing assessment methodology-the new generation,” *ISOPE International Ocean and Polar Engineering Conference*, ISOPE, pp. ISOPE-I-09-062, 2009.
- [4] M. S. Kim, S. B. Kwon, S. K. Kim, J. H. Kim, and J. M. Lee, “Impact failure analysis of corrugated steel plate in LNG containment cargo system,” *Journal of Constructional Steel Research*, vol. 156, pp. 287-301, 2019.
- [5] W. Darmawan, D. Nandika, Y. Massijaya, A. Kabe, I. Rahayu, L. Denaud, and B. Ozarska, “Lathe check characteristics of fast growing sengon veneers and their effect on LVL glue-bond and bending strength,” *Journal of Materials Processing Technology*, vol. 215, pp. 181-188, 2015.
- [6] T. Wang, Y. Wang, R. Crocetti, and M. Wälinder, “In-plane mechanical properties of birch plywood,” *Construction and Building Materials*, vol. 340, 127852, 2022.
- [7] Y. Wang, T. Wang, R. Crocetti, and M. Wälinder, “Experimental investigation on mechanical properties of acetylated birch plywood and its angle-dependence,” *Construction and Building Materials*, vol. 344, 128277, 2022.
- [8] T. Wang, Y. Wang, R. Crocetti, and M. Wälinder, “Influence of face grain angle, size, and moisture content on the edgewise bending strength and stiffness of birch plywood,” *Materials & Design*, vol. 223, 111227, 2022.
- [9] I. Jungerstam, Experimental investigation of the rolling shear properties of birch timber, Master's thesis, *Building Technology*, Aalto University, Finland, 2023.
- [10] J. -H. Kim, S. -W. Choi, D. -H. Park, S. -B. Park, S. -K. Kim, K. -J. Park, and J. -M. Lee, “Effects of cryogenic temperature on the mechanical and failure characteristics of melamine-urea-formaldehyde adhesive plywood,” *Cryogenics*, vol. 91, pp. 36-46, 2018.
- [11] J. -M. Choi, H. -T. Kim, T. -W. Kim, D. -H. Lee, J. -H. Kim, and J. -M. Lee, “Analysis of the compressive behavior of plywood under seawater and cryogenic temperature effects,” *Materials*, vol. 18, no. 8, 1836, 2025.
- [12] Y. -J. Jeong, H. -T. Kim, J. -H. Kim, S. -K. Kim, and J. -M. Lee, “Analysis of glass fiber reinforced composites in Membrane-Type LNG cargo containment system for structural safety using experimentally defined mechanical properties,” *Composite Structures*, vol. 276, 114532, 2021.
- [13] C. -S. Lee, M. -S. Chun, M. -H. Kim, J. -M. Lee, “Debonding failure characteristics of multi-laminated bonding system under cryogenic temperature,” *International Journal of Adhesion and Adhesives*, vol. 31, no. 4, pp. 226-237, 2011.
- [14] Z. Wang, J. Zhou, W. Dong, Y. Yao, and M. Gong, “Influence of technical characteristics on the rolling shear properties of cross laminated timber by modified planar

shear tests,” *Maderas. Ciencia y tecnología*, vol. 20, no. 3, pp. 469-478, 2018.